Binding of β-Amyloid (1–42) Peptide to Negatively Charged Phospholipid Membranes in the Liquid-Ordered State: Modeling and Experimental Studies

Hasna Ahyayauch,[†] Michal Raab,[‡] Jon V. Busto,[†] Nagore Andraka,[†] José-Luis R. Arrondo,[†] Massimo Masserini,[§] Igor Tvaroska,[‡] and Félix M. Goñi[†]

[†]Unidad de Biofísica (CSIC-UPV/EHU) and Departamento de Bioquímica, Universidad del País Vasco, Bilbao, Spain; [‡]Institute of Chemistry, Slovak Academy of Sciences, Bratislava, Slovakia; and [§]Department of Experimental Medicine, University of Milano Bicocca, Monza, Italy

Supplementary data.

Supplementary Methods

MD Simulations:

The monomeric units of PSM, DMPA, and Chol were built with the Maestro program of the Schrodinger software suite (49), and subsequently fully optimized at the DFT/M06-2X (25) level using the 6-31* basis set (49), with the ESP charges calculated at the same level. Next, a grid of the chosen lipid composition was generated by the translation by 10 Å along the x-, and y-axis, and then mirror-imaged and translated along the z-axis to obtain an initial bilayer model. The final grid comprised 16 translated units along the x-, and y-axis, yielding 512 lipids altogether. The monomeric units in the grid were placed in a mass-weighted random order to correspond to the desired lipid compositions PSM:Chol:DMPA (%) of 50:50:0 in model A, 47.5:47.5:5 in model B and 40:40:20 in model C. All systems were solvated with a 60 Å water shell along the z-axis. The negative charge of the membrane was neutralized by the addition of sodium ions up to 0.1M NaCl.

For the minimization, equilibration, and MD simulation of the membrane models, the GROMACS 4 program package (50) was used. A combination of the force field parameters developed by Tieleman (51) and the GROMOS 96 (27) generic parameters was used for the description of PSM and DMPA. For the PSM, the topology for the dipalmitoylphosphatidylcholine (DPPC) developed by Tieleman (51) was modified by the addition of the OH group parameters with the OA (partial charge -0.40) and H (partial charge +0.40) atom types from the GROMACS ffgmx.atp. The parameters of the double bond on the PSM lipidic tail were defined, and the planarity and the trans conformation were achieved by defining an improper torsion angle. For DMPA, the same DPPC topology was modified by removing the choline group and capping the phosphate oxygen with a hydrogen atom (partial charge +0.40). Similar approaches for the development of the force field parameters for PSM and DMPA have been used before (33, 52). For Chol, the parameters developed by Hoeltje et al. in conjunction with the Berger parameters were used (53), and the water molecules were described by the SPC model.

The equilibration of the membrane model consisted of several steps: first, the system was energy minimized for 50000 steps using the steepest descent algorithm to avoid steric clashes. Then, a short 100 ps MD simulation in the NVT ensemble was performed, followed by 20 ns in a NPT ensemble. The system was coupled to the heat bath of 300K using the Nose-Hoover thermostat. The cutoff for the Coulomb interactions was set to 12 Å and the long-range electrostatics was treated by the Particle Mesh Ewald method. A standard leap-frog algorithm was used for the propagation of the simulation with an integration step of 2 fs, while constraining the bond lengths using the LINCS algorithm (54). After 20 ns of the MD run, the potential energy and the dimensions of the box have stabilized and the system was considered equilibrated.
To set up the initial structure used of Aβ42/lipid bilayer for MD simulations, one Aβ42 molecule was added to the each equilibrated bilayer model at an approximate minimum distance of 0.4 nm from the lipid bilayer. Subsequently, the Aβ42/lipid complex was solvated with the SPC water molecules and neutralized by the addition of NaCl ions. The total number of water molecules varied between 25 598 and 37 990, and ion numbers varied between 175 and 251. The exact ion count depends on the size of the

system and on the amount of negatively-charged residues in the simulation box: 75 Na^+ and 75 Cl^- ions have been added to achieve the 0.1M NaCl concentration and 3 Na^+ ions have been added to neutralize the -3 charge on the Aβ42 peptide in all simulations. Furthermore, 22 and 98 Na^+ ions have been added in the simulations B and C respectively, on the account of the single negative charge on the DMPA molecules. The GROMOS 96 force field parameters (27) were applied for the Aβ42 peptide, and the lipid parameters were based on the modified Tieleman (51) force field parameters as described above. Electrostatic interactions were calculated with the Particle Mesh Ewald algorithm. The resulting complex containing between 97 848 and 134 120 atoms was firstly energy minimized to eliminate steric contacts. Subsequently, the Aβ42/lipid was equilibrated in two MD runs under the NVT and NPT ensemble conditions for 100 ps and 1 ns, respectively, while restraining the Aβ42 atoms. After that, a 100 ns production MD in the NPT ensemble was performed with no restraints on any of the models. The constant pressure of 1 bar was applied using the Parinello-Rahman model with semi isotropic coupling (independent scaling along the vector perpendicular to thelipid surface). A standard leap-frog algorithm was used for the propagation of the simulation with an integration step of 2 fs, while constraining the bond lengths using the LINCS algorithm. For all simulations, the GROMACS 4 package (50) was used, and the VMD viewer (51) was used to monitor the simulation results.

Experimental Studies

Preparation of large unilamellar vesicles (LUV)

For liposome preparation, phospholipids were dissolved in chloroform/methanol (2:1, v/v), and the mixture was evaporated to dryness under a stream of nitrogen. Traces of solvent were removed by evacuating the samples under high vacuum for at least 2 h. The samples were hydrated in Tris buffer, helping dispersion by stirring with a glass rod. The solution was frozen in liquid nitrogen and thawed 10 times. LUV were prepared by the extrusion method (29), using polycarbonate filters with a pore size of 0.1 μm (Nuclepore, Pleasanton, CA).

Isothermal Titration Calorimetry (ITC)

ITC was performed using a model VP-ITC high sensitivity titration calorimeter (MicroCal, Northampton, MA). In this study the calorimetric cell was filled with Aβ solution at 28 μM. Lipid vesicles at a 35 mM lipid were injected into the cell (1.43 mL) in 10 μL steps, i.e., leading to a 100–200-fold dilution of lipid vesicles. To minimize the contribution of dilution to the heat of partitioning, both the lipid vesicles and the Aβ solution were prepared in the same buffer and were degassed under vacuum immediately before use. Typically, the injections were made at 10 min intervals and at 2 s/μL. Constant stirring speed of 290 rpm was maintained during the experiment to ensure proper mixing after each injection. Titration experiments were performed at 37°C in Tris buffer. Dilution heats of lipid vesicles into the buffer were determined in separate experiments and subtracted from experimental heats of binding. At each lipid injection, free Aβ monomers partitioned into the bilayer membrane and the corresponding heat of reaction was measured. The heat of reaction became smaller as less and less Aβ remained free in solution. The integration of each calorimetric peak yields a heat of reaction. These heats were plotted versus the lipid concentration.

Lipid monolayer measurements

Monomolecular layers at the air-water interface in a Langmuir balancewere studied at 22 °C using a μTrough-S equipment (Kibron, Helsinki, Finland) consisting on a small 2-cm rounded multi-well plate that allowed for 1 mm subphase measurements. Monolayers were formed by spreading a small amount of lipid (about 2 nmol) in chloroform:methanol (2:1, v/v) solution over tris buffer. After allowing for solvent evaporation, Aβ was added to the subphase through an adjusted hole. Pure Aβ monolayers were built by injecting this peptide into the subphase without previous lipid spreading, following the Aβ transition to the interface in terms of changes in surface pressure. Aβ 42 stock solution was 50μM. Aβ 42 final concentration in the trough was 1.22μM.

Thioflavin T (ThT) assay. We used the ThT assay for determination of β-sheet content and this has been often used as a semi-quantitative indication of β-sheet formation by Aβ42. Briefly, ThT was prepared in glycine (50 mM, pH 8.2) and filtered (0.22 mm). Stock Aβ42 was added to each vesicle solution to yield incubation mixtures containing 5 μM Aβ with 1:200 peptide to lipid mole ratio at 37˚C. ThT was then added. Following gentle mixing, the fluorescence was recorded in an Aminco-Bowman (Urbana, IL) AB-2 spectrofluorometer (λex=446 nm, λem=485 nm). Control samples of pure Aβ and peptide-free vesicles were also prepared and measured as indicated.

Infrared spectroscopy measurements. Samples were recorded in a Nicolet Nexus 5700 (Madison, WI, USA) spectrometer equipped with a MCT detector using a Peltier cell (TempCon, Bio Tolls, Inc., Florida) with 25 μm carved calcium fluoride windows. Analysis was performed at 37˚C. Samples contained 80 μM Aβ42, at a 1:200 peptide lipid mole ratio. Spectra were collected using a rapid scan software under OMNIC, supplied by Nicolet. Typically, 370 interferograms were collected per spectrum and then referred to a background, the spectra being obtained with a nominal resolution of 2 cm^{-1}.

The physical state of lipid bilayers containing DMPA. SM:Chol (1:1) bilayers are recognised to exist in the liquid-ordered state [see (56) and references therein]. However no data are available, to the authors' knowledge, on the phase behaviour of SM:Chol:DMPA compositions. For this reason the SM:Chol:DMPA (40:40:20, mol ratio) mixture was examined by fluorescence microscopy, differential scanning calorimetry (DSC) and fluorescence spectroscopy (laurdan generalised polarisation). These techniques indicate clearly that the SM:Chol:DMPA bilayers under study are in the liquid-ordered phase. Pure egg PC bilayers exist in the liquid-disordered phase (56). Addition of DMPA does not promote a measurable phase change, as indicated by laurdan fluorescence spectroscopy

Differential Scanning Calorimetry

For DSC, both the lipid suspension and buffer were degassed before being loaded into the sample or reference cell of an MC-2 high-sensitivity scanning calorimeter (MicroCal, Northampton, MA). The final lipid concentration was 2 mM. Three heating scans, at 45 ˚C/h were recorded for each sample. After the first one, successive heating scans on the same sample always yielded superimposable thermograms. Transition temperatures,

enthalpies, and widths at half-height were determined using the software ORIGIN (MicroCal) provided with the calorimeter.

GUV preparation and fluorescence microscopy
GUVs were prepared using the electroformation method developed by Montes et al. (57). Stock solutions of lipids (0.2 mg/ml total lipid containing 0.2 mol% DiI) were prepared in a chloroform-methanol (2:1, v/v) solution. Three microliters of the appropriate stocks were added to the surface of Pt electrodes, and solvent traces were removed by evacuating the chamber under high vacuum for at least 2 h. Then, the Pt electrodes were covered with 400 µl of 10 mM HEPES buffer (pH 7.4), previously heated to 60°C. The Pt wires were connected to an electric wave generator (TG330 function generator; Thurlby Thandar Instruments, Huntington, UK) under AC field conditions (frequency 10 Hz; amplitude, 1 V) for 2 h at 60°C. After GUV formation, the chamber was placed on an inverted confocal fluorescence microscope (D-Eclipse C1 model; Nikon Inc., Melville, NY). The excitation wavelength for DiI was 561 nm. The observations were performed at room temperature. Image treatment and quantification were performed using EZ-C1 version 3.20 software (NikonInc., Melville, NY).

Fluorescence Polarization Assays.
The generalized polarization (GP) of laurdan was measured with SLM 8100 spectrofluorometer. The excitation GP_{EX} parameter was calculated according to
$GP_{EX} = (I_{440} - I_{490})/(I_{440} + I_{490})$

where I_{440} and I_{490} are the intensities at each excitation wavelength from 325 to 410 nm obtained using fixed emission wavelengths of 440 and 490 nm, respectively. The final probe/lipid molar ratio was 1/1000.

Supplementary Results
The physical state of SM:Chol:DMPA bilayers
A preliminary study was addressed to describe the physical state of the bilayers used in this study. For this purpose, SM:Chol (1:1) and SM:Chol:DMPA (40/40/20) bilayers were used, the former being well-known representatives of a lamellar phase in the liquid-ordered phase. GUV of bilayers containing 20% DMPA were stained with DiI. This probe partitions preferentially into the liquid-disordered phase when the latter coexists with the liquid-ordered phase. However our GUV (Supplementary Figure S5 A) show a homogeneous distribution of DiI in the vesicles, indicating that no phase coexistence was taking place. The possibility of a gel phase present even in the form of very small domains was precluded by the DSC data in Fig. S5 B. Neither in the presence nor in the absence of 20 mol% DMPA was there a gel-fluid transition detected by calorimetry. Finally, the laurdan generalized polarization data in Fig S5 C, for LUVs composed of SM:Chol (1:1) and for SM:Chol:DMPA (40:40:20) demonstrate that both mixtures exist at room temperature in the form of liquid-ordered bilayers (58).

Egg PC bilayers are known to exist in the liquid-disordered phase at and above room temperature. Laurdan generalized polarization confirms this (Fig. S5 D) and shows that addition of DMPA up to 20 mol% at room temperature does not cause a major phase change.

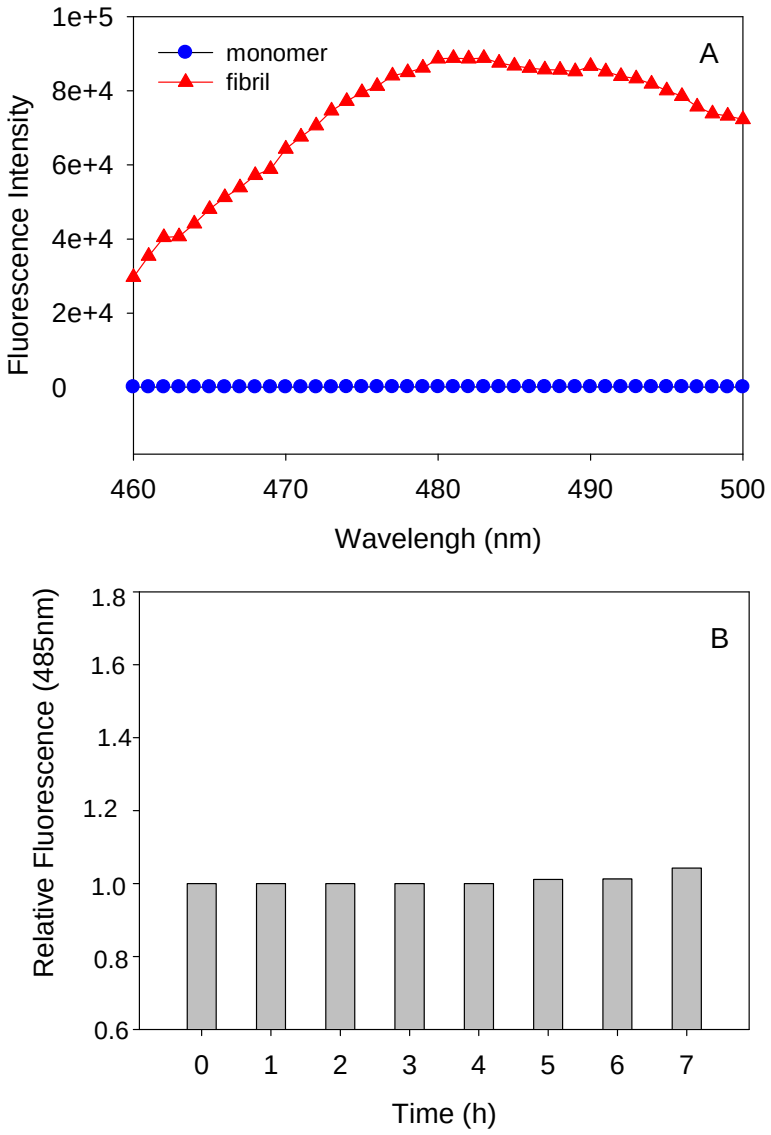
A
monomer
fibril
Fluorescence Intensity
1e+5
8e+4
6e+4
4e+4
2e+4
0
460
470
480
490
500
Wavelengh (nm)
B
Relative Fluorescence (485nm)
1.8
1.6
1.4
1.2
1.0
0.8
0.6
0
1
2
3
4
5
6
7
Time (h)

Fig. S1

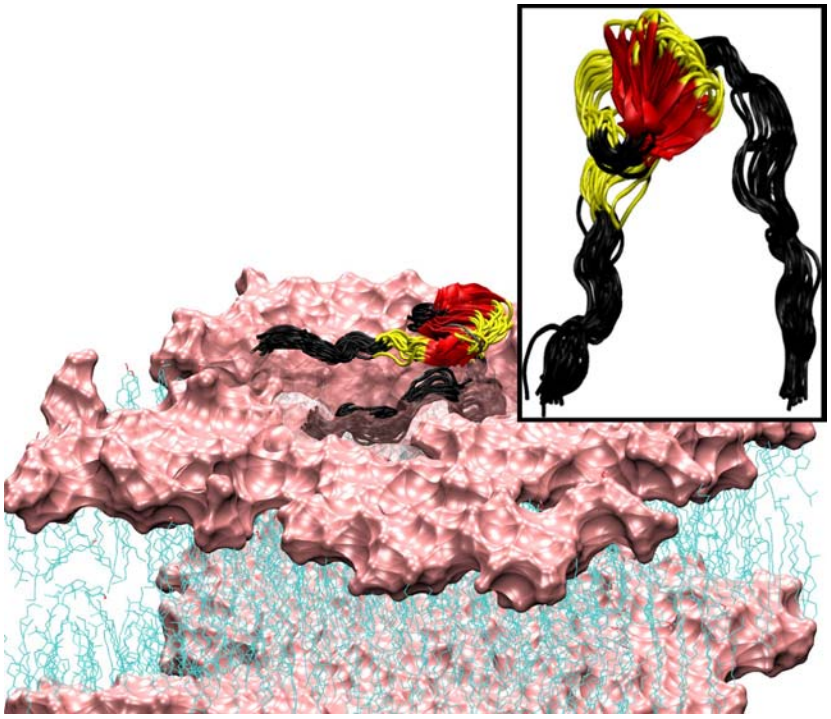

A

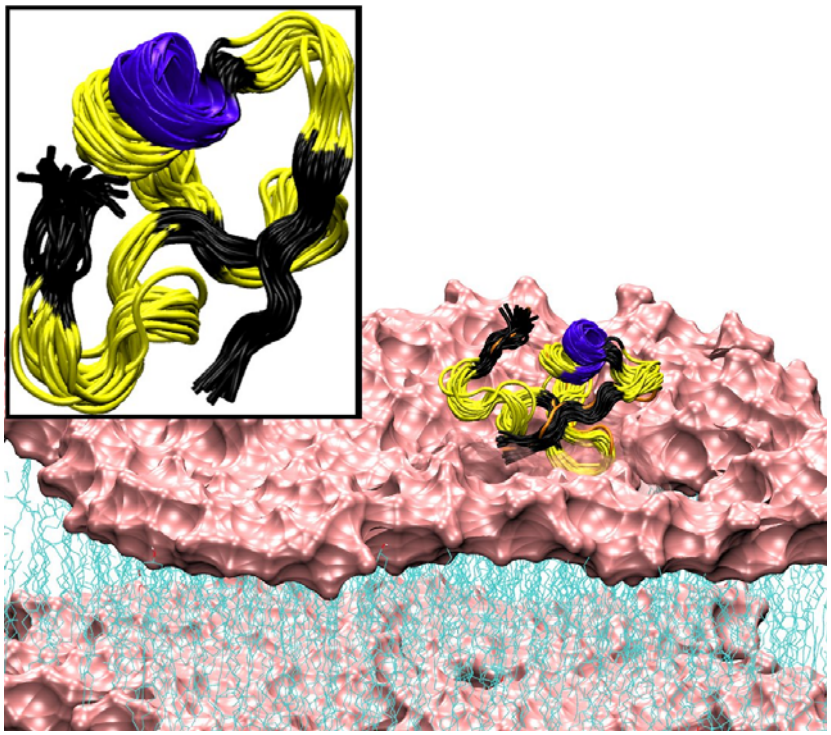

B

Figure S2

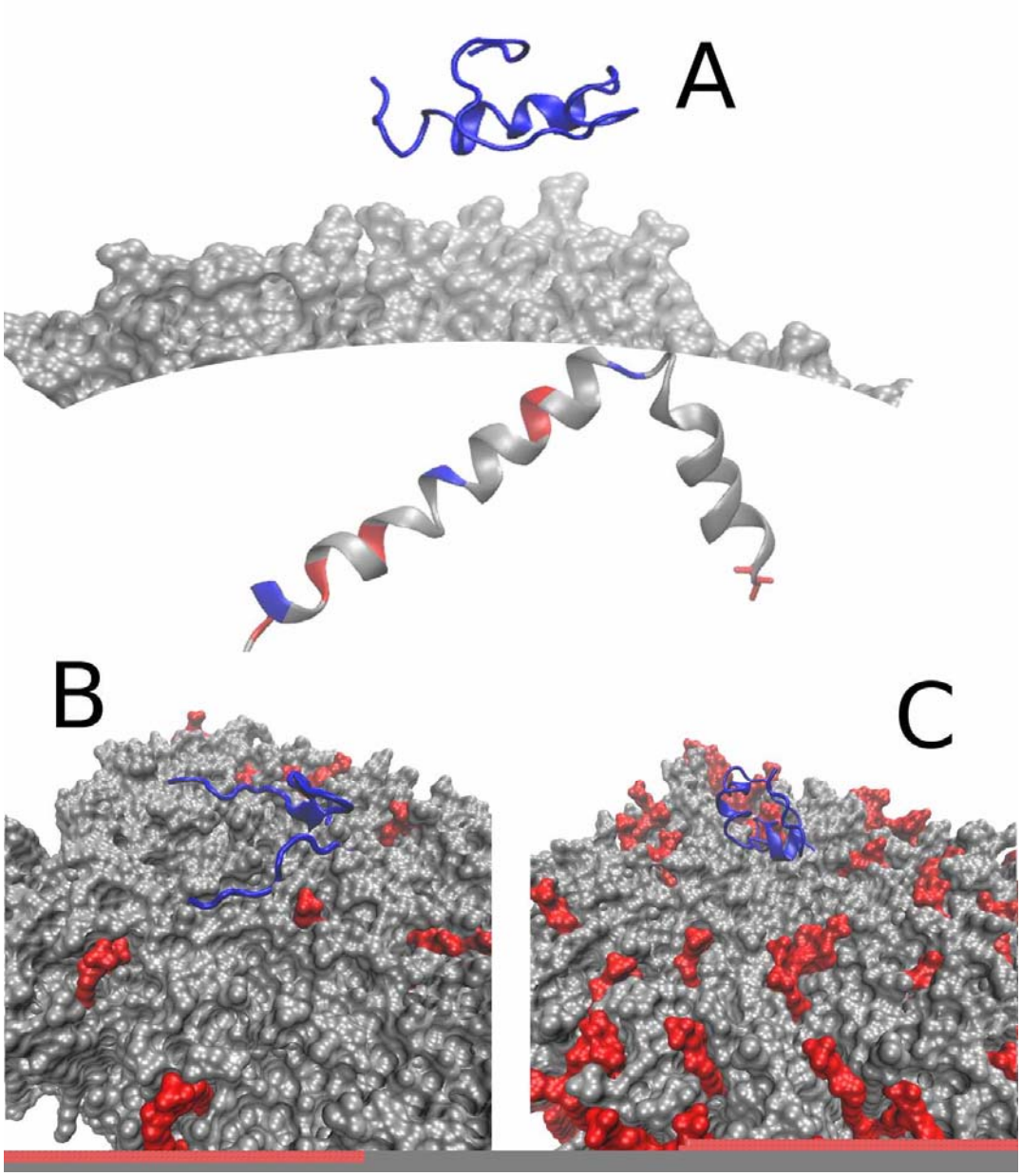

Figure S3

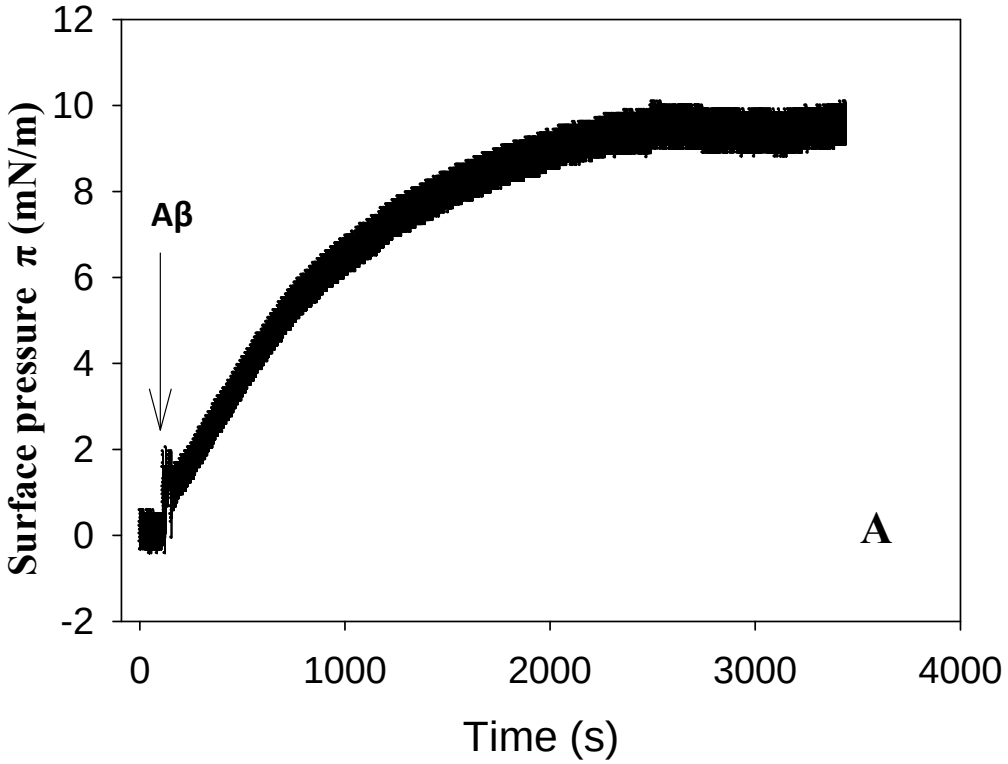
Surface pressure π (mN/m)
Aβ
A
Time (s)

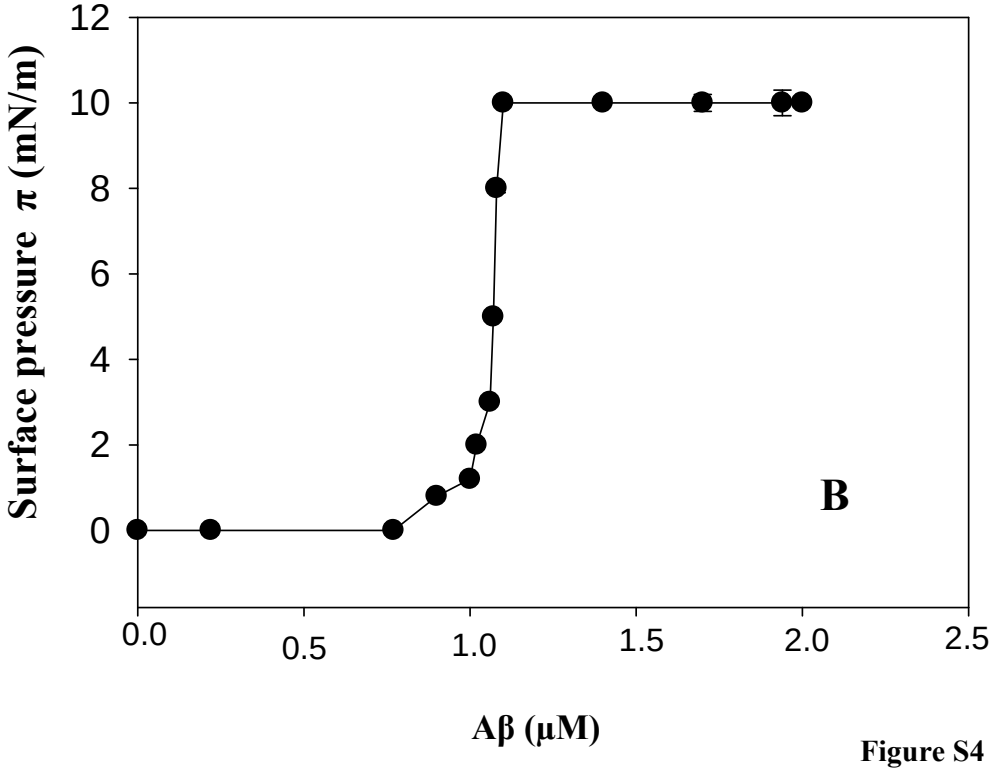
Surface pressure π (mN/m)
B
Aβ (μM)

Figure S4

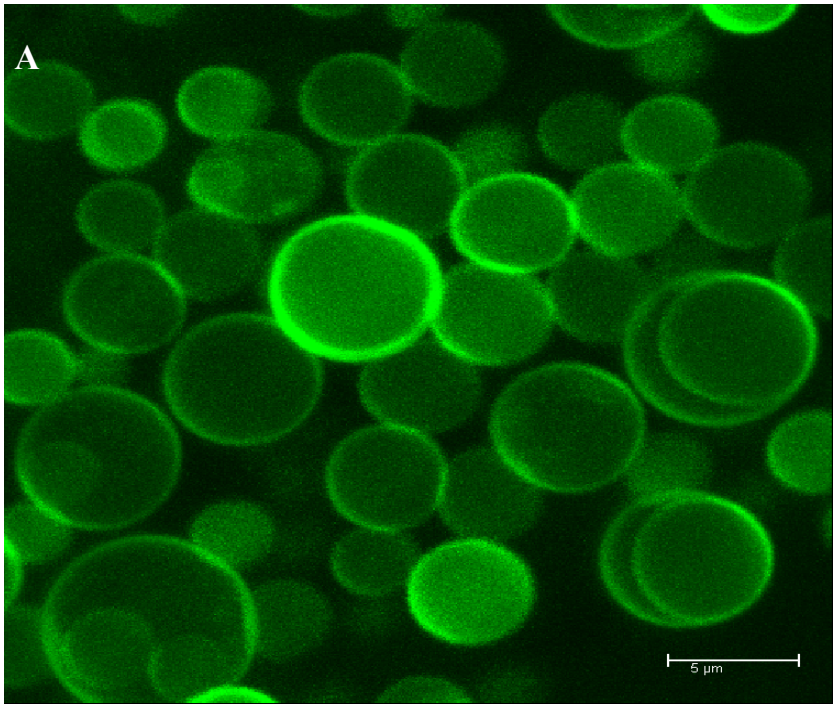
A
5 µm

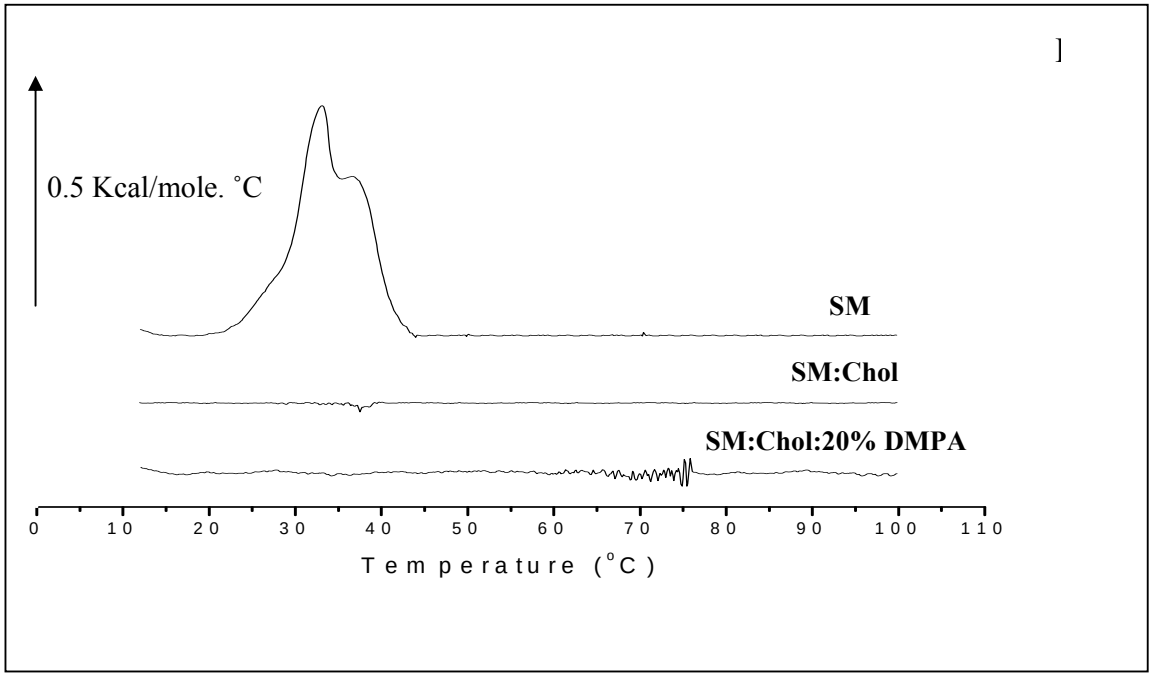
0.5 Kcal/mole. ˚C
SM
SM:Chol
SM:Chol:20% DMPA
0 10 20 30 40 50 60 70 80 90 100 110
Temperature (°C)

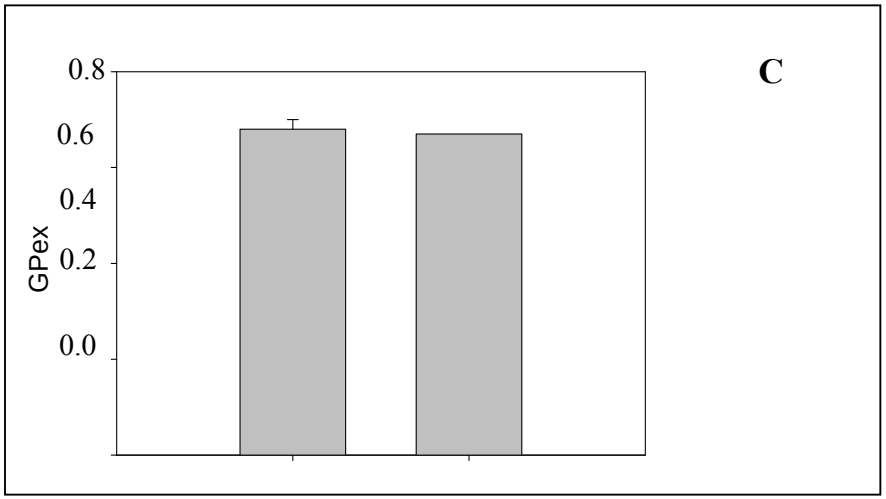
C
0.8
0.6
0.4
0.2
0.0
GPex
SM:Chol
SM:Chol:20%DMPA

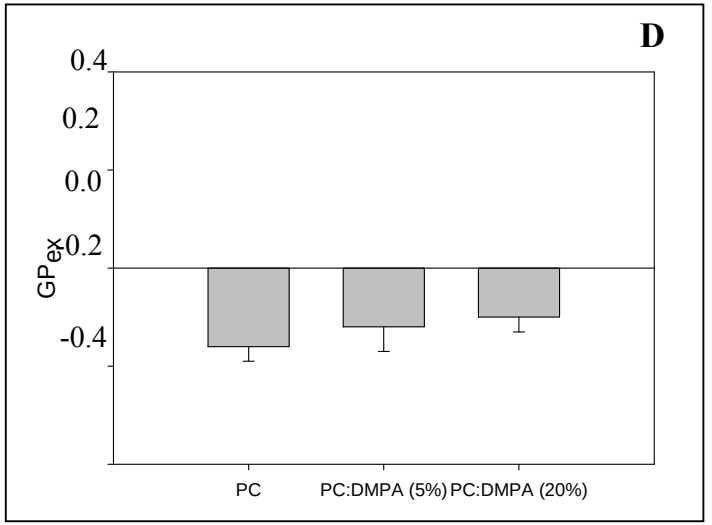
D
0.4
0.2
0.0
-0.2
-0.4
GPex
PC
PC:DMPA (5%)
PC:DMPA (20%)

Figure

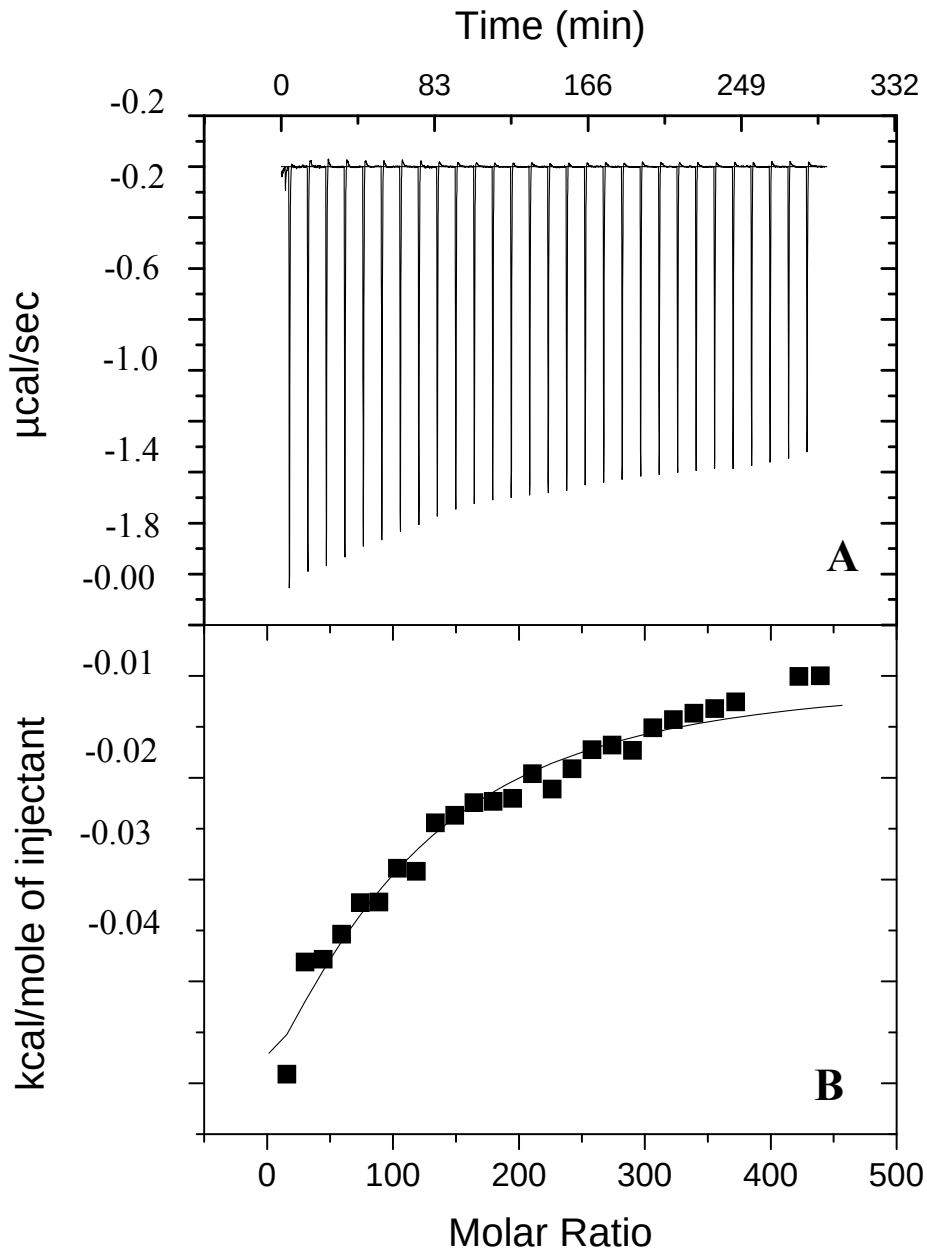
Time (min)
0
83
166
249
332
-0.2
-0.2
-0.6
-1.0
-1.4
-1.8
-0.00
µcal/sec
A
-0.01
-0.02
-0.03
-0.04
kcal/mole of injectant
B
0
100
200
300
400
500
Molar Ratio

Figure S6

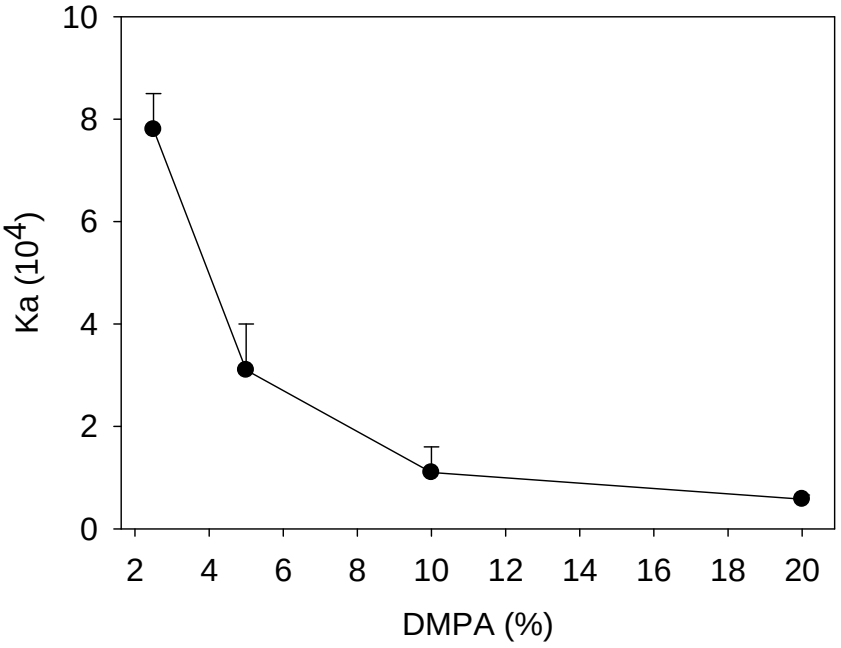

Figure. S7

Supplementary Figure S1: Aβ42 is in the monomeric form under the conditions of our experiments. A, thioflavin T fluorescence emission spectra in the presence of Aβ42 in the monomer (●) or fibril (▲) form. When required Aβ42 in fibril form was prepared in a pH2 buffer (59), and incubated at 37˚C for 48h. B, time course of thioflavin T fluorescence emission in the presence of monomeric Aβ42. Aβ 42 final concentration was 5μM.

Supplementary Figure S2. Visualization of the Aβ42 cluster binding to the membrane surface in models B and C. The secondary structure of the peptide is color coded as follows: black - coil, yellow - turn, red - β-sheet, blue-helix.

Supplementary Figure S3. The snapshot of the Aβ42 structures bound on the A, B, and C bilayer models, respectively. The negatively charged DMPA lipids on bilayers are colour-coded red; negatively charged residues of Aβ42, are in red, and positively charged residues in blue.

Supplementary Figure S4. Aβ 42-induced changes in surface pressure at an air–water interface. (A) Time course of a representative experiment, at 1.22 μM peptide concentration. (B) Equilibrium values obtained from experiments as shown in panel A, as a function of peptide concentration. Average values ± S.E.M (n=3).

Supplementary Figure S5: Membranes composed of SM:Chol:DMPA are in the fluid ordered state. A, confocal microscopy of GUV (SM:Chol:DMPA, 40:40:20), stained with DiI. The uniform staining reveals the lack of phase separation. Bar = 5μm. B, differential scanning calorimetry thermograms of pure SM, SM:Chol (1:1), or SM:Chol:DMPA (40:40:20). The lack of transition in the two lower thermograms indicates that no gel phase is present. C, generalised polarisation of laurdan. LUV of different compositions as indicated by each bar. The mixture containing 20% DMPA appears to be largely in the fluid-ordered phase. D, laurdan generalised polarisation of bilayers based on egg PC and Egg PC/DMPA mixtures, as indicated by each bar. Average values ± S.E:M: (n=3).

Supplementary Figure S6. Titration calorimetry of LUV composed of SM/Chol/DMPA (47.5/47.5/5) with Aβ 42 monomers. The titration experiments were performed at 37˚C. (A) Heat exchange in successive vesicle injections. (B) Molar heat exchange as a function of lipid:peptide molar ratio. Data collected from a representative experiment. Average data are summarized in Table 1.

Supplementary Figure S7. The variation in association constant (Ka) of Aβ 42 to LUV composed of SM/Chol (1/1) plus increasing concentrations of DMPA. Calorimetric data derived from Table 1.

References

49. Zhao, Y., and D.G. Truhlar. 2008. Density functionals with broad applicability in chemistry. Acc. Chem. Res. 41: 157–167.

50. Hess, B., C. Kutzner, D. van der Spoel, and E. Lindahl. 2008. GROMACS 4: Algorithms for highly efficient, load-balanced, and scalable molecular simulation. J. Chem. Theory Comput. 4: 435–447.

51. Tieleman, D. P., and H.J.C. Berendsen. 1996. Molecular dynamics simulations of fully hydrated dipalmitoylphosphatidylcholine bilayer with different macroscopic boundary conditions and parameters. J. Chem. Phys. 105: 4871–4880.

52. Cheng, M. H., L.T. Liu, A.C. Saladino, Y. Xu, and P. Tang. 2007. Molecular dynamics simulations of ternary membrane mixture: phosphatidylcholine, phosphatidic acid, and cholesterol. J. Phys. Chem. B 111: 14186–14192.

53. Höltje, M., T. Förster, B. Brandt, T. Engels, W. von Rybinski, and H. D. Höltje. 2001. Molecular dynamics simulations of stratum corneum lipid models: fatty acids and cholesterol. Biochim. Biophys. Acta. 1511: 156–167.

54. Hess, B., H. Bekker, H. Berendsen, and J.J. Fraaije. 1997. A Linear Contstraint Solver for Molecular Simulations. J. Comput. Chem. 18: 1463–1472.

55. Humphrey, W., A. Dalke, and K.J. Schulten. 1996. Visual molecular dynamics. Mol. Graphics Modell. 14: 33–38, 27–38.

56. Goñi, F.M., A. Alonso, L.A. Bagatolli, R.E. Brown, D. Marsh, M. Prieto, and J.L. Thewalt. 2008. Phase diagrams of lipid mixtures relevant to the study of membrane rafts. Biochim. Biophys. Acta. 1781: 665–684

57. Montes, L.R., A. Alonso, F.M. Goñi, and L.A. Bagatolli. 2007. Giant unilamellar vesicles electroformed from native membranes and organic lipid mixtures under physiological conditions. Biophys. J. 93:3548–3554.

58. Parasassi, T., G. De Stasio, G. Ravagnan, R.M. Rusch, and E. Gratton. 1991. Quantitation of lipid phases in phospholipid vesicles by the generalized polarization of Laurdan fluorescence. Biophys. J. 60:179–189.

59. Dahlgren, K.N., A.M. Manelli, Jr. W.B. Stine, L. K. Baker, G. A. Krafft, and M. J. LaDu. 2002. Oligomeric and fibrillar species of amyloid-beta peptides differentially affect neuronal viability. J. Biol. Chem. 277: 32046–32053.